THE JOURNAL OF BIOLOGICAL CHEMISTRY
Vol. 278, No. 20, Issue of May 16, pp. 18281–18288, 2003

Printed in U.S.A.

Structure-to-Function Relationship of Mini-Lipoxygenase, a 60-kDa Fragment of Soybean Lipoxygenase-1 with Lower Stability but Higher Enzymatic Activity*

Received for publication, November 27, 2002, and in revised form, February 5, 2003
Published, JBC Papers in Press, March 7, 2003, DOI 10.1074/jbc.M212122200

Almerinda Di Venere‡§, Maria Luisa Salucci¶, Guus van Zadelhoff‖, Gerrit Veldink‖, Giampiero Mei‡§, Nicola Rosato‡§, Alessandro Finazzi-Agrò§, and Mauro Maccarrone‡‡§§**

*From the ‡INFM, 16152 Genova, Italy, the §Department of Experimental Medicine and Biochemical Sciences, University of Rome, Tor Vergata, 00133 Rome, Italy, the ¶Department of Pure and Applied Biology, University of L'Aquila, 67100 L'Aquila, Italy, ‖Bijvoet Center for Biomolecular Research, Department of Bio-organic Chemistry, Utrecht University, 3584 CH Utrecht, The Netherlands, **AFaR-CRCCS Divisione di Neurologia, Ospedale San Giovanni Calibita, Fatebenefratelli, 00100 Rome, Italy, and the ‡‡Department of Biomedical Sciences, University of Teramo, 64100 Teramo, Italy*

Lipoxygenase-1 (Lox-1) is a member of the lipoxygenase family, a class of dioxygenases that take part in the metabolism of polyunsatured fatty acids in eukaryotes. Tryptic digestion of soybean Lox-1 is known to produce a 60 kDa fragment, termed "mini-Lox," which shows enhanced catalytic efficiency and higher membrane-binding ability than the native enzyme (Maccarrone, M., Salucci, M. L., van Zadelhoff, G., Malatesta, F., Veldink, G. Vliegenthart, J. F. G., and Finazzi-Agrò, A. (2001) *Biochemistry* 40, 6819–6827). In this study, we have investigated the stability of mini-Lox in guanidinium hydrochloride and under high pressure by fluorescence and circular dichroism spectroscopy. Only a partial unfolding could be obtained at high pressure in the range 1–3000 bar at variance with guanidinium hydrochloride. However, in both cases a reversible denaturation was observed. The denaturation experiments demonstrate that mini-Lox is a rather unstable molecule, which undergoes a two-step unfolding transition at moderately low guanidinium hydrochloride concentration (0–4.5 M). Both chemical- and physical-induced denaturation suggest that mini-Lox is more hydrated than Lox-1, an observation also confirmed by 1-anilino-8-naphthalenesulfonate (ANS) binding studies. We have also investigated the occurrence of substrate-induced changes in the protein tertiary structure by dynamic fluorescence techniques. In particular, eicosatetraynoic acid, an irreversible inhibitor of lipoxygenase, has been used to mimic the effect of substrate binding. We demonstrated that mini-Lox is indeed characterized by much larger conformational changes than those occurring in the native Lox-1 upon binding of eicosatetraynoic acid. Finally, by both activity and fluorescence measurements we have found that 1-anilino-8-naphthalenesulfonate has access to the active site of mini-Lox but not to that of intact Lox-1. These findings strongly support the hypothesis that the larger hydration of mini-Lox renders this molecule more flexible, and therefore less stable.

Lipoxygenases (Loxs)[1] form a homologous family of non-heme, non-sulfur iron containing lipid-peroxidizing enzymes, which catalyze the dioxygenation of polyunsatured fatty acids to the corresponding hydroperoxy derivatives. Mammalian Loxs have been implicated in the pathogenesis of several inflammatory conditions such as arthritis, psoriasis, and bronchial asthma (1). They are also thought to have a role in atherosclerosis, brain aging, human immunodeficiency virus infection, kidney diseases, and terminal differentiation of keratinocytes, because they are key enzymes in the arachidonate cascade, together with cyclooxygenases (2). In plants, lipoxygenases are active in germination, in the synthesis of traumatin and jasmonic acid, and in the response to abiotic stress (3). Recently, Lox activity has been shown to be instrumental in inducing irreversible damages to organelle membranes (4–5), a process that might be the basis for the critical role of Loxs in programmed cell death induced by various pro-apoptotic stimuli (6). The biological activities of Loxs have attracted a growing interest on both their functional and structural properties. Plant and mammalian Loxs are made by a single polypeptide chain folded in a two-domain structure (7). The N-terminal domain is a β-barrel of ~110–115 (mammals) and 150 (plants) residues, whereas the larger C-terminal domain is mainly helical and contains the catalytic site.

Soybean lipoxygenase-1 (Lox-1) is widely used as a prototype for studying the structural and functional properties of lipoxygenases from tissues of different species (7). Lox-1 has a 30-kDa N-terminal domain and a 60-kDa C-terminal domain containing the catalytically active iron and the substrate-binding pocket. The function of the N-terminal β-barrel domain has been elusive for several years, for Lox-1 as well as for other Loxs (7). Recently, the N-terminal domain has been shown to be essential for calcium binding and activation of 5-lipoxygenase activity (8) and for nuclear membrane translocation of this Lox isoform (9–10). Equilibrium unfolding experiments on Lox-1 have shown that the C-terminal domain is less stable than the N-terminal domain, undergoing chemical denaturation in the early steps of the complex protein unfolding process (11). The smaller N-terminal domain seems to retain a large part of its β-barrel structure even at high urea concentration, suggesting that this portion of the protein structure might be important for the overall protein stability. Limited proteolytic cleavage of Lox-1 into the N- and C-terminal do-

* This study was supported in part by grants from Istituto Superiore di Sanità (IV AIDS project), Agenzia Spaziale Italiana (contract I/R/098/00), Ministero dell'Instruzione, dell'Università e della Ricerca (COFIN 2001), and the Consiglio Nazionale delle Ricerche target projects MADESS II and Ministero Politiche Agricole e Forestali (progetto FORMINNOVA 2002), Rome. The costs of publication of this article were defrayed in part by the payment of page charges. This article must therefore be hereby marked "*advertisement*" in accordance with 18 U.S.C. Section 1734 solely to indicate this fact.

§§ To whom correspondence should be addressed. Tel.: 39-0861-266875; Fax: 39-0861-412583; E-mail: Maccarrone@vet.unite.it.

[1] The abbreviations used are: Lox, lipoxygenase; GdHCl, guanidinium hydrochloride; CD, circular dichroism; ETYA, eicosatetraynoic acid; ANS, 1-anilino-8-naphthalenesulfonate.

FIG. 1. **Three-dimensional structure of mini-Lox.** Ribbon model of mini-Lox obtained from the Lox-1 crystallographic file (Protein Data Bank code 2sbl) removing the first 277 aminoacids. The 12 trypthophan residues are evidenced.

mains, and their subsequent isolation, have added new important structural and functional information (12). In particular, the electrophoretic, chromatographic, and spectroscopic analyses of the purified 60-kDa C-terminal domain of Lox-1 (termed "mini-Lox") have shown that the trimmed enzyme is still folded. Surprisingly, mini-Lox was shown to have a greater catalytic activity than intact Lox-1, thus suggesting a built-in inhibitory role for the N-terminal domain (12). In addition, mini-Lox displayed a higher binding affinity than Lox-1 for artificial membranes, attributable to the enhanced surface hydrophobicity exposed after removal of the 30-kDa N-terminal fragment. Interestingly, similar results have been recently reported about the effect of the N-terminal domain removal on the activity and membrane-binding ability of the reticulocyte-type 15-lipoxygenase (13).

A three-dimensional representation of mini-Lox can be generated from the Lox-1 crystallographic data (Fig. 1). The high number of trypthophans (12) renders this enzyme spectroscopically very complex, as demonstrated by the great heterogeneity of the mini-Lox fluorescence spectrum (12). A somewhat greater solvent accessibility of aromatic chromophores of mini-Lox with respect to Lox-1 is apparent probably associated to a conformational change after proteolytic cleavage (12).

In our study we have investigated the relationship between the activity of mini-Lox (*e.g.* enhanced enzymatic activity) and its structural features checked by circular dichroism, 1-anilino-8-naphthalenesulfonate (ANS) binding, steady-state, and dynamic fluorescence. Because the balance between the loss of hydrophobic interactions and the enhanced solvation upon the N-terminal removal is crucial to understand the mini-Lox properties, we have also studied the stability of mini-Lox using complementary techniques, such as chemical equilibrium unfolding measurements and denaturation by hydrostatic pressure. The results demonstrate that the removal of the N-terminal domain makes the mini-Lox more sensitive to denaturation by both guanidinium hydrochloride (GdHCl) and pressure. Furthermore, dynamic fluorescence measurements and ANS binding experiments provide new evidence that the active site is more accessible in the mini-Lox than in the Lox-1 and that quite different conformational changes follow the substrate binding in the two enzymes. All together these results provide a new structural rationale that might explain the peculiar mini-Lox features.

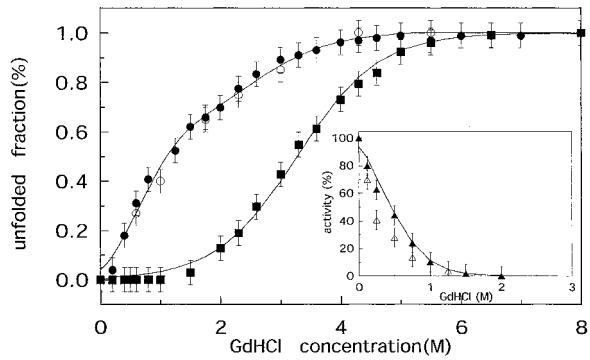

FIG. 2. **Denaturation of mini-Lox by GdHCl.** The denaturation at different GdHCl concentrations was monitored by steady-state fluorescence (λ_{ex} = 280 nm, *filled circles*; λ_{ex} = 295 nm, *open circles*) and CD at 220 nm (*squares*). *Solid lines* represent the best fit obtained using a three-state (fluorescence) or two-state (CD) denaturation model (Table I). In the *inset* the mini-Lox enzymatic activity is reported as a function of GdHCl (*filled triangles*). The activity recovered upon refolding is instead indicated by *empty symbols*.

EXPERIMENTAL PROCEDURES

Materials and Enzymes—Linoleic (9,12-octadecadienoic) acid and 5,8,11,14-eicosatetraynoic acid (ETYA) were purchased from Sigma. Ultrapure guanidinium hydrochloride and ANS were purchased from US Biochemical Corp. and Molecular Probes Inc., respectively. Lipoxygenase-1 (linoleate:oxygen oxidoreductase, EC 1.13.11.12; Lox-1) was purified from soybean (*Glycine max* [L.] Merrill, Williams) seeds as reported (14), and mini-Lox was prepared as previously described (12). Briefly, Lox-1 was digested with trypsin at a Lox-1/trypsin 10:1 (w/w) ratio, which allowed completion of the reaction within 30 min. Chromatographic separation of the tryptic fragments was performed by high performance liquid chromatography gel-filtration on a Biosep-SEC-S3000 column (600 × 7.8 mm, Phenomenex, Torrance, CA). Fractions corresponding to the 60-kDa fragment eluted after 10 min as a single peak, and were pooled, dialyzed against water, and concentrated on Centricon 30 ultrafiltration units (Amicon, Beverly, MA) (12). This 60-kDa fragment, referred to as mini-Lox, was found to be electrophoretically pure on 12% SDS-polyacrylamide gels, and its N-terminal amino acid analysis showed the sequence STPIEFHSFQ, which corresponds to a unique trypsin cleavage site between lysine 277 and serine 278 (12). Such a cleavage should indeed remove a 30-kDa N-terminal domain of Lox-1, leading to a fragment of the expected molecular mass of 63,695 Da (12). Protein concentration was determined according to Bradford (15), using bovine serum albumin as a standard. Dioxygenase activity of mini-Lox in 100 mM sodium borate buffer (pH 9.0) was assayed spectrophotometrically at 25 °C by recording the formation of conjugated hydroperoxides from linoleic acid at 234 nm (16). Except for lifetime measurements, all the experiments were performed dissolving Lox-1 and mini-Lox in 0.1 M Tris-HCl buffer (pH 7.2) at a final protein concentration of 1.5 μM. For lifetime measurements, Lox-1 and mini-Lox were used at 10 μM, to obtain a good signal to noise ratio.

Equilibrium Unfolding Measurements—Protein denaturation by GdHCl was obtained after a 12 h incubation at 4 °C in the presence of different amounts of denaturant. Fluorescence and CD spectra were recorded at 20 °C after 30 min of incubation. Unfolding and refolding pathways were independent of protein concentration. Refolding of fully unfolded mini-Lox samples was achieved by diluting the denaturant concentration with buffer. The analysis of the unfolding transition was performed as described elsewhere (17), according to a two step denaturation pathway according to Scheme 1,

$$N \overset{K_1}{\leftrightarrow} I \overset{K_2}{\leftrightarrow} U$$

SCHEME 1

where N, I, and U represent the native, intermediate, and unfolded protein fractions. They were directly evaluated as a linear combination from the fluorescence signal. K_1 and K_2 are the two equilibrium constants related to the respective free energy values ΔG_1 and ΔG_2, which are supposed to vary linearly with the denaturant concentration [D] as shown in Equation 1 (where i = 1.2).

$$\Delta G_i = \Delta G_{H_2O} - m[D] \qquad \text{(Eq. 1)}$$

TABLE I
Physical Parameters Characterizing the Unfolding of Mini-Lox

The parameters have been obtained by fitting CD, enzymatic activity, and fluorescence data (Figs. 2 and 3) according to a two- or three-state denaturation process (see "Experimental Procedures"). The errors on the calculated parameters were directly obtained by the fitting routine.

Mini-Lox unfolding by GdHCl	ΔG_1	m_1	ΔG_2	m_2	ΔG_{TOT}	$[D]_{½}$
	kcal/mol	*kcal/molM*	*kcal/mol*	*kcal/molM*	*kcal/mol*	*M*
Fluorescence	1.5 ± 0.1	2.0 ± 0.1	2.5 ± 0.2	1.0 ± 0.1	4.0 ± 0.2	
Activity	1.0 ± 0.2	2.2 ± 0.2				0.46
Circular dichroism			2.8 ± 0.2	0.9 ± 0.2		3.20
Mini-Lox unfolding by pressure	ΔG_1	ΔV_1				
	kcal/mol	*ml/mol*				
	1.5 ± 0.1	−69 ± 10				

A non-linear least-squares fit was used to evaluate the parameters reported in Table I, according to the minimum χ^2 value. A single transition model was instead sufficient to fit both the CD and activity data.

Circular Dichroism, Steady-State, and Dynamic Fluorescence Measurements—CD spectra were recorded on a Jasco-710 spectropolarimeter, at 20 °C, using a 0.1 cm quartz cuvette. Steady-state fluorescence spectra have been recorded using an ISS-K2 spectrofluorometer (ISS), at 20 °C upon excitation at 280 nm. No differences were observed in fluorescence spectra when the excitation wavelength was varied from 280 to 295 nm due to a very efficient energy transfer from tyrosines to tryptophans. High pressure measurements were performed with the same instrument, using the high pressure ISS cell equipped with an external bath circulator. The analysis of the high pressure unfolding transition was performed assuming a two-state equilibrium model between native and intermediate species as shown in Equation 2 as follows,

$$N \overset{K_1}{\leftrightarrow} I \qquad \text{(Eq. 2)}$$

with $\Delta G = -RT\ln K_1$ and $\Delta V = (\partial \ln K_1)/\partial P$).

The fluorescence emission decay of both Lox-1 and mini-Lox was extrapolated from the phase-shift and demodulation data, obtained with the cross-correlation technique (18) upon excitation at 280 nm, using the frequency-modulated light of an arc-xenon lamp, in the range 5–200 MHz. The emission was observed through a 305 nm cutoff filter to avoid the contribution of scattered light.

1-Anilino-8-naphthalenesulfonate Binding Measurements—ANS binding was measured as follows. Fluorescence spectra in the range 420–550 nm were recorded as a function of the amount of ANS (λ_{exc} = 350 nm), at fixed protein concentration, then each spectrum was resolved according to the linear combination in Equation 3

$$S_{exp} = C_F S_F + C_B S_B \qquad \text{(Eq. 3)}$$

where S_{exp}, S_F, and S_B are column vectors corresponding to the experimental, ANS-free, and ANS-bound spectra. C_F and C_B represent the extrapolated linear correlation coefficients representing the percentage of free and bound ANS, respectively. The spectrum of the totally bound ANS (S_B) was extrapolated, in a separate experiment, by varying the protein concentration, in the presence of a fixed amount of ANS (19). The ANS binding data have been represented as Scatchard plots and fitted according to models for one or two independent classes of sites (20) as follows,

$$\frac{\nu}{[L]} = \sum_i \frac{n_i k_i}{1 + k_i[L]} \qquad \text{(Eq. 4)}$$

where ν represents the moles of ANS bound per moles of protein, $[L]$ is the concentration of free ANS, i = 1 or 2, and n_i and k_i are the number of binding sites and the association constant of each class of sites. The fits were performed using the SPW 1.0 version of the Sigmaplot scientific graphic software (by Jandel Scientific).

RESULTS AND DISCUSSION

Mini-Lox Is a Rather Unstable Molecule—The stability of mini-Lox has been studied by equilibrium unfolding measurements at increasing GdHCl concentrations (Fig. 2). The non-coincidence of the fluorescence and CD measurements demonstrates that the unfolding transition was not cooperative and that the presence of stable intermediate species had to be taken into account. The simplest denaturation model, which successfully fitted the experimental data, was a three-state process, N ↔ I ↔ U (see "Experimental Procedures"), whose parameters are reported in Table I. As shown by the very early and steep increase of the fluorescence signal (Fig. 2), a small free energy of unfolding (Table I) characterizes the first transition (0–1.5 M GdHCl). No relevant change occurred in the CD signal at low GdHCl concentration, and the data could be fitted according to a two-state model (Table I). The overall stabilization energy obtained from the spectroscopic measurements ($\Delta G^0_{tot} \approx 4.0 \pm 0.3$ kcal/mol) demonstrated that mini-Lox is rather unstable, specially if compared with intact Lox-1 ($\Delta G^0_{tot} \approx 26$ kcal/mol (11)). Combined refolding and proteolysis experiments have suggested that the C-terminal domain of Lox-1 is the less stable part of the intact enzyme. This domain, which roughly corresponds to the whole mini-Lox molecule, is probably fully unfolded in the intermediate state found in the Lox-1 denaturation pathway (11). The transition from the native structure to this intermediate species is characterized by a quite large free energy change ($\Delta G^0_1 \approx 14$ kcal/mol), as compared with the total stabilization energy of mini-Lox (Table I). It can be therefore concluded that the low stability of mini-Lox is due to the removal of the 30-kDa N-terminal domain. As a matter of fact this hypothesis is indirectly supported by the m_i values reported in Table I. The m parameter, which describes the cooperativity of the unfolding process, is strictly correlated to the change in protein-accessible surface area upon denaturation (21). In particular, greater hydration has been found to correspond to larger m values and *vice versa* (21). It is also well known that m values obtained with GdHCl are about 2.2× larger than those obtained with urea (21). Thus, even though different unfolding agents have been used in the equilibrium unfolding measurements of Lox-1 and mini-Lox (urea and GdHCl, respectively), it is possible to compare the different results obtained for the two proteins. In particular, from the results reported by Sudharshan and Appu Rao (11), it can be expected that the GdHCl-induced denaturation of Lox-1 would yield $m_1 \approx 4.4$ kcal/mol M and $m_2 \approx 3.5$ kcal/mol, for the first and second step of its unfolding pathway. On the other hand, the total m value for mini-Lox (Table I) is ≈ 3 kcal/mol, *i.e.* 30% less than that obtained in the first transition of Lox-1. This lower value stands for a smaller change in the solvent-exposed surface area, indicating that the native mini-Lox is more hydrated than the C-terminal domain of Lox-1. Thus, the N-terminal Lox-1 domain plays a fundamental structural role, shielding the other domain from the solvent and therefore enhancing its stability.

Characterization of Mini-Lox Unfolding Intermediate under Hydrostatic Pressure—Despite its low stabilization energy, the mini-Lox unfolding pathway was complex (Fig. 2), suggesting

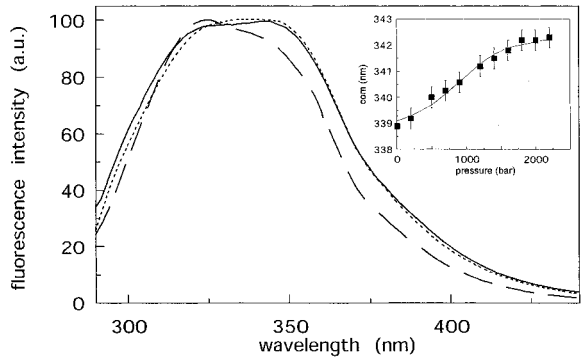

FIG. 3. **High pressure effect on mini-Lox.** Steady-state fluorescence spectra of mini-Lox, native (*dashed line*), partially unfolded in 1.5 M GdHCl (*dotted line*), or at 2400 bar (*solid line*). In the *inset* the center of mass (*com*) of mini-Lox fluorescence spectrum is reported as a function of pressure. The *solid line* represents the best fit obtained with a two-state unfolding model.

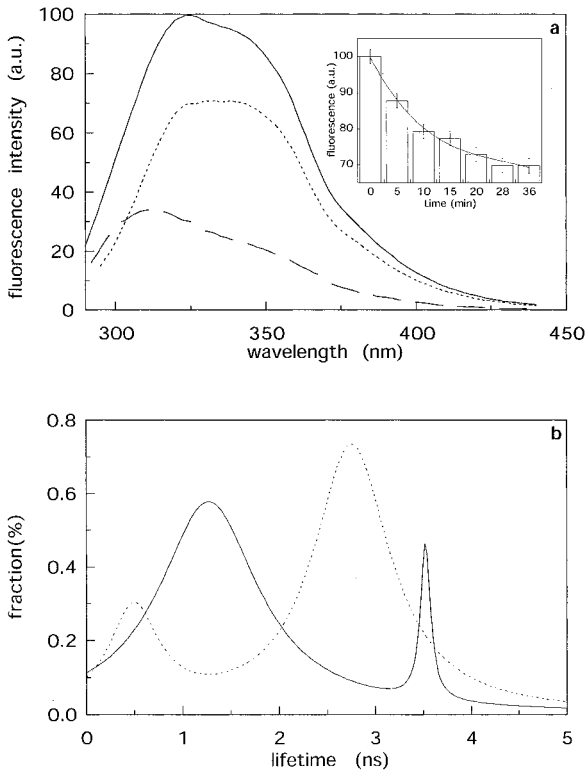

FIG. 4. **ETYA binding to mini-Lox.** *a*, steady-state emission spectra of mini-Lox (*solid line*) and of mini-Lox incubated for 45 min in the presence of 20 molar excess of ETYA (*dotted line*). The *dashed line* is the difference spectrum. The *inset* shows the total fluorescence intensity of mini-Lox as a function of time after addition of ETYA. *b*, fluorescence lifetime distributions of mini-Lox (*solid line*) and of mini-Lox in the presence of 20 molar excess of ETYA after 45 min incubation (*dotted line*).

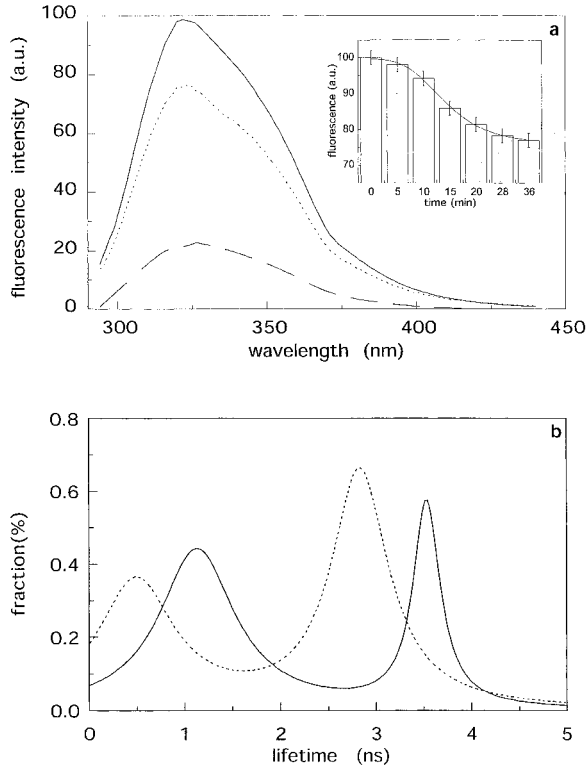

FIG. 5. **ETYA binding to Lox-1.** *a*, steady-state emission spectra of Lox-1 (*solid line*) and of Lox-1 incubated for 45 min in the presence of 20 molar excess of ETYA (*dotted line*). The *dashed line* is the difference spectrum. The *inset* shows the total fluorescence intensity of Lox-1 as a function of time after addition of ETYA. *b*, fluorescence lifetime distributions of Lox-1 (*solid line*) and of Lox-1 in the presence of 20 molar excess of ETYA after 45 min incubation (*dotted line*).

the presence of stable (or partially stable) intermediate species. Measurements of enzymatic activity demonstrated that the protein biological activity was progressively lost between 0 and 1.5 M GdHCl (Fig. 2, *inset*). The corresponding free energy value ($\Delta G \approx 1.0 \pm 0.2$ kcal/mol), very close to that calculated for the first fluorescence phase (Table I), reflects the high instability of the enzyme, especially around the active site region. In fact, in the same range a significant loosening of the protein tertiary structure was taking place, as revealed by the change (50%) of the protein intrinsic fluorescence signal (Fig. 2). These findings suggest that the intermediate state is partially unfolded, but it retains a native-like secondary structure. Such features resemble those of the so-called molten globule state, an unfolding intermediate species described in the denaturation pathway of several globular proteins (22–23). The most relevant property of this structure is indeed a greater exposure of the protein hydrophobic moieties to the solvent. In the case of mini-Lox, the great heterogeneity of the fluorescence spectrum (12), due also to a high number of tryptophan residues (Fig. 1), makes it impossible to dissect the contribution of each domain to the fluorescence of the intermediate state. In the last years, several studies have demonstrated that molten globule intermediates may be also produced by hydrostatic pressure, which may force solvent into the protein core (24).

Fig. 3 reports the fluorescence spectra of mini-Lox at 1 and 2400 bar. A shift of the emission signal toward longer wavelengths at higher pressure values is observed (Fig. 3, *inset*), supporting the hypothesis of a progressive hydration of the internal tryptophylic residues. It almost perfectly overlaps the steady-state spectrum in the presence of 1.5 M GdHCl (Fig. 3), demonstrating that physically induced unfolding may neatly reproduce chemical denaturation. Actually, the two-state fit reported in the *inset* of Fig. 3 yields the same free energy of unfolding (≈ 1.5 kcal/mol) characterizing the first denaturation transition in GdHCl (Table I). The corresponding volume change has also been evaluated (see "Experimental Procedures") and resulted to be quite small (-69 ± 9 ml/mol), despite the large protein size ($\approx$ 63,000 Da) as usually found by compression of globular proteins (24–25). Recent studies on the pressure-induced molten globule state of cytochrome *c* (26), α-lactalbumin (27), apomyoglobin (28), and the Ras domain of RalGDS (29) reported ΔV values from 15 to 70 ml/mol, quite similar to that found here for mini-Lox, which, however, is a

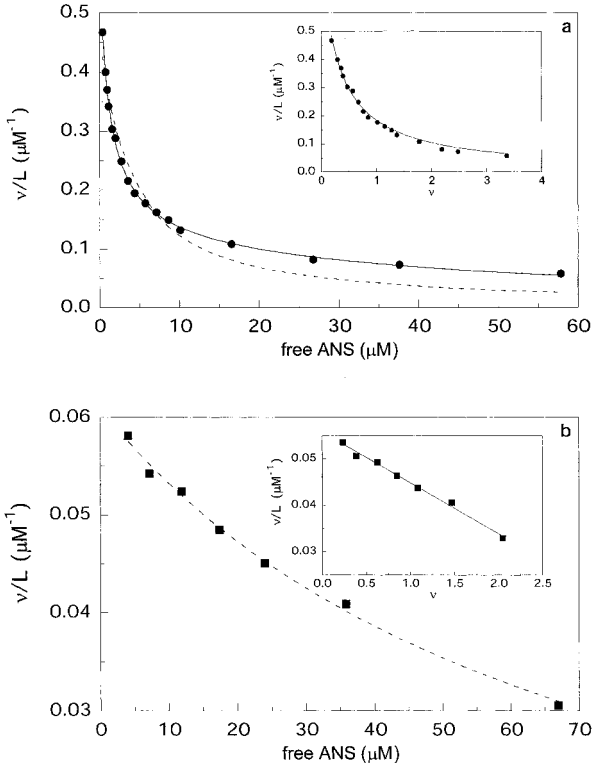

FIG. 6. **ANS binding to mini-Lox.** *a*, Scatchard plot for ANS binding to mini-Lox. The two fits were obtained using a single class of equivalent binding sites (*dashed line*, with $n_1 \approx 2$, $k_1 \approx 3 \times 10^5$ M^{-1}) or two different classes of ANS-binding sites (*solid line*, with $n_1 \approx 1$, $k_1 \approx 9 \times 10^5$ M^{-1} and $n_2 \approx 4$, $k_2 \approx 2 \times 10^4$ M^{-1}). In the *inset* the data have been reported as a function of ANS moles bound per mole of mini-Lox to highlight the presence of a biphasic behavior. *b*, Scatchard plot for ANS binding to mini-Lox-ETYA complex. The fit was obtained using a single class of equivalent binding sites (*solid line*, with $n \approx 4$, $k \approx 1.4 \times 10^5$ M^{-1}). In the *inset* the data have been reported as a function of ANS moles bound per mole of mini-Lox to highlight the presence of a linear behavior.

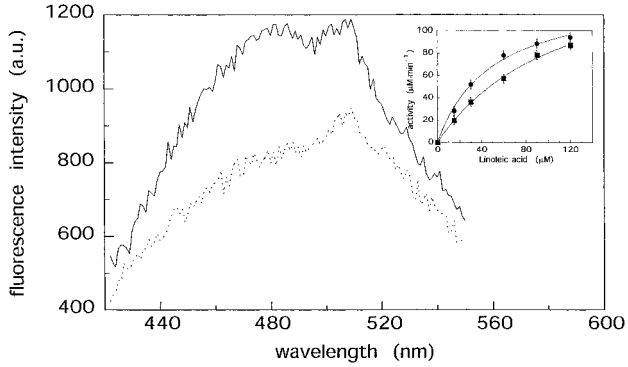

FIG. 7. **Effects of ETYA on ANS binding to mini-Lox.** *Solid line*, fluorescence spectrum of ANS bound to mini-Lox after 30 min incubation (at a ANS to mini-Lox ratio of 5:1). *Dotted line*, the measurement was repeated by previously reacting mini-Lox with ETYA (20-fold excess). In the *inset* the dependence on substrate concentration of the dioxygenation of linoleic acid by mini-Lox (*circles*) and mini-Lox in the presence of 2 molar excess of ANS (after 30 min incubation, *squares*) is reported.

much larger molecule. In this line, the results obtained with point mutants of staphylococcal nuclease (30) have suggested that the collapse of internal cavities under pressure might be the main source of the volume changes. Because the number and size of cavities in a protein have been found to be related to its molecular weight (31–33), the low ΔV value obtained for mini-Lox could be explained by assuming that most protein cavities are already solvated at ambient pressure. Not only this hypothesis is consistent with the chemical denaturation experiments, but it could also explain the easier resiliency of mini-Lox with respect to Lox-1. In fact, at variance with the native enzyme (11, 34–35), both pressure and GdHCl unfoldings of mini-Lox were fully reversible, being activity, CD, and fluorescence spectra fully recovered after restoring the initial conditions.

Mini-Lox Conformational Changes upon ETYA Binding—Because mini-Lox is more active but less stable than Lox-1, we have investigated which conformational changes were involved in the biological activity. To this aim, both steady-state and dynamic fluorescence measurements were performed in the presence of ETYA, an irreversible inhibitor of lipoxygenase that rapidly binds at the active site (36).

Normalized steady-state spectra of mini-Lox and Lox-1 in the presence and absence of ETYA are reported in Figs. 4*a* and 5*a*, respectively. The decrease in the emission intensity indicated that ETYA strongly quenches the intrinsic fluorescence of both proteins, yet the overall effect was remarkably different in the two cases. First of all, as revealed by the peak position (≈325 nm) and the full width at half-maximum, the spectral shape of Lox-1 spectrum did not change after incubation for 30 min in the presence of the inhibitor. The difference spectrum was symmetrical and centered at the same wavelength (≈325 nm), indicating that quenching is affecting in the same way both exposed and buried tryptophans. Instead, the fluorescence spectrum of mini-Lox appeared to be red-shifted and narrowed in the presence of ETYA (Fig. 4*a*). The difference spectrum, peaking around 315 nm, was diagnostic of a preferential quenching of the less hydrated tryptophylic residues in the protein. It is worth mentioning that the drop in fluorescence intensity following ETYA addition was not sudden, but required almost 30 min to reach equilibrium for both proteins (see *insets* of Figs. 4*a* and 5*a*). This finding strongly suggests that the quenching mechanism must be indirect, probably due to an induced protein conformational change upon ETYA binding. As a matter of fact, spectroscopic (37–38), structural (39), and chemical denaturation studies (40) have shown that some (1–3) tryptophylic residues are essential for the enzymatic activity of Lox-1, located in the hydrophobic substrate-binding site. Thus, a simple diffusion of ETYA into the active site would have led to a much faster quenching process than observed for both proteins (*insets* of Figs. 4*a* and 5*a*). Interestingly, the time course of this process was not the same in the two proteins: the fluorescence intensity of mini-Lox decreased exponentially, whereas much slower kinetics were observed in the case of Lox-1 (*insets* of Figs. 4*a* and 5*a*). One possible explanation for this different behavior might be the larger degrees of freedom experienced by the mini-Lox molecule. Thus, larger conformational changes might be expected for mini-Lox upon ETYA binding.

This hypothesis has been checked by dynamic fluorescence measurements, which are in fact extremely sensitive to changes in the protein tertiary structure (41). The fluorescence decay of large, multi-tryptophan-containing proteins is heterogeneous and generally best described by continuous distributions of lifetimes, rather than by few discrete components (42–44). Previous measurements have shown that the dynamic fluorescence of Lox-1 may be resolved into a pair of lorentzian lifetimes distributions, probably associated to two distinct classes of tryptophylic residues, depending on their relative exposure to the solvent molecules (35). In the present study the phase and demodulation technique (18) has been used to characterize the fluorescence decay of mini-Lox and Lox-1 upon excitation at 280 nm. The results, shown in Figs. 4*b* and 5*b*,

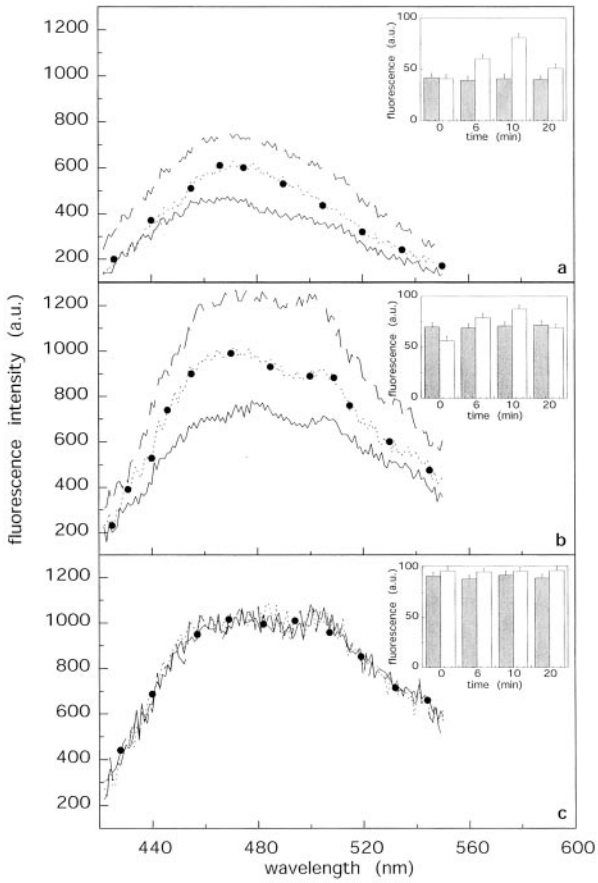

FIG. 8. **Fluorescence kinetics of ANS binding.** Time-dependence of the ANS fluorescence spectrum change upon binding to mini-Lox. The ANS to protein ratio was 0.6:1 (*panel a*), 2:1 (*panel b*), or 4:1 (*panel c*). *Solid*, *dashed*, *dotted lines*, and *circles* correspond to spectra recorded at 0, 10, 20, and 30 min, respectively. In the *insets* the time-dependence of the ANS fluorescence intensity upon binding to Lox-1 (*filled bars*) and mini-Lox (*empty bars*) is reported.

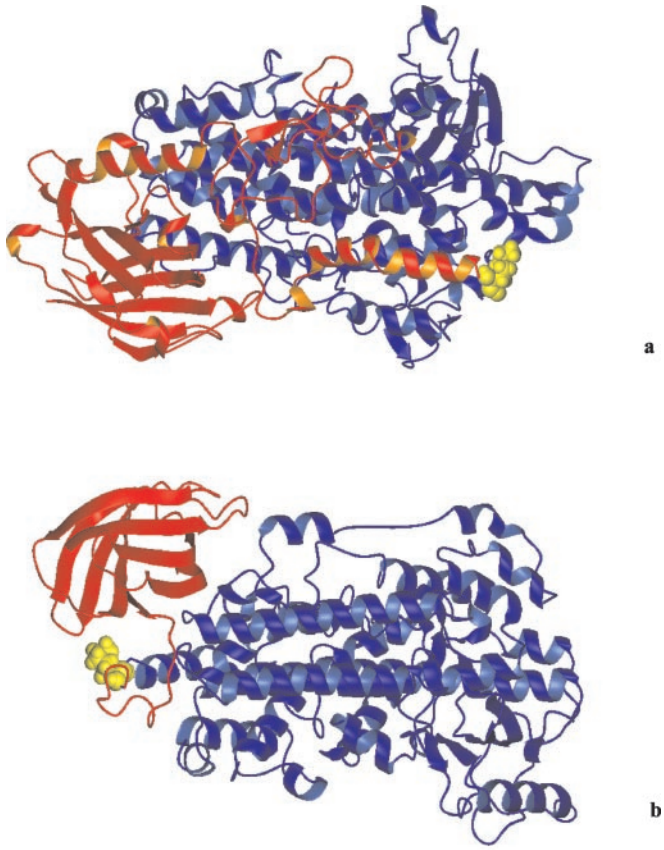

FIG. 9. **Three-dimensional structure of soybean Lox-1 and of rabbit 15-lipoxygenase.** *a*, ribbon model of Lox-1 (Protein Data Bank code 2sbl) shown in *red* the N-terminal domain removed by trypsin digestion and in *blue* in the remaining C-terminal fragment (mini-Lox). The trypsin cleavage site (lysine 277) is shown in *yellow*. *b*, ribbon model of 15-lipoxygenase (Protein Data Bank code 1lox) shown in *red* the N-terminal domain and in *blue* in the remaining C-terminal fragment. The site of a possible trypsin cleavage (lysine 127) is shown in *yellow*.

demonstrate that in both cases a double distribution is required to fit the experimental data. Despite the peak positions being quite similar (*i.e.* $c_1 \approx 1.25$ ns and $c_2 \approx 3.5$ ns), the relative fractional intensities were inverted for mini-Lox (*i.e.* F_1 was greater than F_2). This result rules out the possibility that the short-lived component was essentially due to tryptophans located in the N-terminal domain of Lox-1, as previously suggested by urea unfolding measurements (35). The average lifetimes, evaluated from the distribution analysis of Lox-1 and mini-Lox, were $\tau_{\text{Lox-1}} \approx 1.18$ ns and $\tau_{\text{mini-Lox}} \approx 1.00$ ns, respectively, indicating a 20% more efficient dynamic quenching in the case of mini-Lox. This result could be indeed expected for a more solvated structure, as suggested for mini-Lox (see above). The analysis of the dynamic fluorescence measurements performed in the presence of ETYA yielded very similar distribution profiles (Figs. 4*b* and 5*b*), characterized by an overall shift toward shorter lifetimes and a marked decrease in the fractional intensity of the first component, F_1. The last effect was more evident for mini-Lox and paralleled the asymmetrical change of the fluorescence spectrum upon ligand binding (Fig. 4*a*). In conclusion, kinetics, steady-state and dynamic fluorescence measurements point to the occurrence of larger conformational changes in the tertiary structure of mini-Lox than of Lox-1.

ANS Binding Experiments—ANS is a well known fluorescent probe, whose quantum yield considerably increases upon binding to hydrophobic pockets of proteins. Its emission spectrum also depends on the environment, being blue-shifted the deeper and tighter its interaction with the protein matrix (45). Hence ANS is a very suitable probe to investigate the formation of protein-fatty acids complexes (46–47). Previous measurements on Lox-1 have demonstrated that the native enzyme has one binding site for ANS and that the enzymatic activity is not inhibited by the fluorescent probe (48). It was therefore concluded that ANS does not interact with the fatty acid-binding site, but rather interacts with another hydrophobic patch present in the protein structure. The above reported unfolding measurements and spectroscopic assays of mini-Lox have pointed out that the main structural differences between the two enzymes are associated with the solvent accessibility, at the level of their tertiary structure. We have therefore analyzed the binding of ANS to the protein. Fig. 6*a* reports the Scatchard plot for ANS binding to mini-Lox, showing a clear biphasic behavior indicative of the presence of multiple binding sites. Because no evidence for cooperativity was obtained by other procedures (*e.g.* Hill plots), the data were fitted according to models taking into account one or two different classes of independent binding sites (see "Experimental Procedure"). This last fit gave the best results (Fig. 6*a*), with one and four binding sites for the two classes, respectively, hence confirming that the mini-Lox surface is characterized by a larger number of hydrophobic patches than Lox-1. The association constants of the two classes (Fig. 6*a*) were largely different (the first one being 50 times greater than the second), indicating that the single site had enhanced affinity for ANS. At variance with Lox-1, a significant reduction of the enzymatic activity was

obtained in the presence of ANS (Fig. 7, *inset*), suggesting that some kind of interaction between the probe and the protein active site was possibly taking place. To check this possibility another approach was used, *i.e.* measuring the spectrum of ANS after the mini-Lox active site was occupied by the irreversible inhibitor ETYA. The results demonstrated that the occupancy of the active site by ETYA reduced the ANS fluorescence by about 22% (Fig. 7), suggesting that the two molecules compete for the mini-Lox catalytic site. This hypothesis has been further tested by performing a titration of ANS binding to the mini-Lox-ETYA complex. In this case the linearity of the Scatchard plot (Fig. 6*b*) is a clear indication of similar binding sites. Indeed, a fit of the data yielded four identical, low affinity binding sites (Fig. 6*b*). This finding allows us to identify the higher affinity ANS-binding site found in the absence of ETYA with the enzyme active site. No effect of ETYA on the ANS binding was observed in control experiments performed with Lox-1 (data not shown).

Kinetic measurements of ANS binding to both mini-Lox and Lox-1 revealed another interesting difference between the two enzymes (Fig. 8). As shown in Fig. 8, *a* and *b*, the change of ANS fluorescence signal upon binding to mini-Lox was rather slow, requiring 15–20 min to reach equilibrium. This time-dependence was observed only at low ANS/protein ratios, namely between 0.6:1 (Fig. 8*a*) and 2:1 (Fig. 8*b*). In these cases the ANS fluorescence intensity changes are probably due to re-arrangements of the protein tertiary structure, and in particular to fluctuations in the polarity of the ANS-binding site.

No time dependence was detected in the case of Lox-1, at any ANS concentration (Fig. 8, *a*, *b*, and *c*, *insets*). Interestingly, the time course characterizing ANS fluorescence changes was the same found for ETYA binding, indicating that similar conformational changes might be induced in the protein tertiary structure to allow their access into the active site.

CONCLUSIONS

The fact that mini-Lox, the 60-kDa fragment of Lox-1, is more efficient than the whole native protein in both dioxygenase activity and membrane-binding ability (12) is rather intriguing. In this paper we attempted to figure out which possible correlation holds between biological and structural features of mini-Lox. We have shown that the removal of the 30-kDa fragment from the 90-kDa molecule generates a more hydrated protein, which displays an increased affinity for hydrophobic probes like ANS. Mini-Lox appears to undergo larger conformational changes than Lox-1 upon ETYA and ANS binding, displaying greater sensitivity but also better reversibility after pressure- and GdHCl-induced unfolding. It could be argued that a larger structural flexibility due to the partial loosening of the tertiary structure is the main reason for the enhanced activity. In particular, the possibility of binding ANS in the active site is a direct evidence that mini-Lox gives the substrates an easier access to the hydrophobic cavity, where the catalysis takes place. In this context, the hypothesis that the N-terminal domain of Lox-1 could act as a built-in inhibitor of the enzymatic activity (12) takes ground. It seems noteworthy that trypsin-trimmed Lox-1, as well as "reconstituted" Lox-1 obtained by adding the tryptic fragments of molecular mass <60 kDa to mini-Lox, showed the same activity as isolated mini-Lox, suggesting that these <60 kDa fragments had no effect on enzyme activity (12). This result is at variance with a previous report (49). On the other hand, an inhibition of mini-Lox by these fragments could be expected, in view of the enhanced activity of the trimmed enzyme compared with the native form. It can be proposed that the lack of effect (either stimulatory or inhibitory) of the <60 kDa fragments on mini-Lox activity simply reflects a different interaction between the N-terminal and C-terminal fragments after proteolysis. In addition, the N-terminal fragment could also make the native enzyme less able to bind hydrophilic molecules, and more selective toward hydrophobic molecules like its natural lipid substrates. By the way soybean Lox-1 is a 15-lipoxygenase (7) and interestingly its mammalian counterpart, *i.e.* the rabbit reticulocyte 15-lipoxygenase, has a similar site for trypsin cleavage (50). The C-terminal domain generated by a cleavage at this site would have almost the same size (535 *versus* 562 amino acid residues) and an overall structure like mini-Lox (Fig. 9). Furthermore, the C-terminal domain of rabbit 15-lipoxygenase is similar to that of human 5-lipoxygenase (51). Therefore, it is tempting to speculate that what was found with mini-Lox might hold true also for mammalian lipoxygenases, and that the trimmed enzymes might play a role in physio(patho)logical conditions, where enhanced lipoxygenase activity and membrane lipoperoxidation have been observed, such as kidney disease in humans (52) and programmed cell death in animals (6) and plants (53). Noteworthy, in the latter organisms, a trypsin-like protease, termed SNP1, has been shown to be expressed during infection by pathogens (54), a typical situation where lipoxygenase is known to be activated (55).

REFERENCES

1. Kühn, H., and Borngraber, S. (1999) *Adv. Exp. Med. Biol.* **447,** 5–28
2. Funk, C. D. (2001) *Science* **294,** 1871–1875
3. Grechkin, A. (1998) *Prog. Lipid Res.* **37,** 317–352
4. van Leyen, K., Duvoisin, R. M., Engelhardt, H., and Wiedmann, M. (1998) *Nature* **395,** 392–395
5. Grullich, C., Duvoisin, R. M., Wiedmann, M., and van Leyen, K. (2001) *FEBS Lett.* **489,** 51–54
6. Maccarrone, M., Melino, G., and Finazzi-Agrò, A. (2001) *Cell Death Differ.* **8,** 776–784
7. Brash, A. R. (1999) *J. Biol. Chem.* **274,** 23679–23682
8. Hammarberg, T., Provost, P., Persson, B., and Radmark, O. (2000) *J. Biol. Chem.* **275,** 38787–38793
9. Chen, X. S., and Funk, C. D. (2001) *J. Biol. Chem.* **276,** 811–818
10. Jones, S. M., Luo, M., Healy, A. M., Peters-Golden, M., and Brock, T. G. (2002) *J. Biol. Chem.* **277,** 38550–38556
11. Sudharshan, E., and Appu Rao, A. G. (1999) *J. Biol. Chem.* **274,** 35351–35358
12. Maccarrone, M., Salucci, M. L., van Zadelhoff, G., Malatesta, F., Veldink, G. Vliegenthart, J. F. G., and Finazzi-Agrò, A. (2001) *Biochemistry* **40,** 6819–6827
13. Walther, M., Anton, M., Wiedmann, M., Fletterick, R., and Kühn H. (2002) *J. Biol. Chem.* **277,** 27360–27366
14. Finazzi-Agrò, A., Avigliano, L., Veldink, G. A., Vliegenthart, J. F. G., and Boldingh, J. (1973) *Biochim. Biophys. Acta* **326,** 462–470
15. Bradford, M. M. (1976) *Anal. Biochem.* **72,** 248–254
16. Schilstra, M. J., Veldink, G. A., and Vliegenthart, J. F. G. (1994) *Biochemistry* **33,** 3974–3979
17. Di Venere, A., Rossi, A., Rosato, N., De Matteis, F., Finazzi-Agrò, A., and Mei, G. (2000) *J. Biol. Chem.* **275,** 3915–3921
18. Gratton, E., and Limkeman, M. (1983) *Biophys. J.* **44,** 315–324
19. Cardamone, M., and Puri, N. K. (1992) *Biochem. J.* **282,** 589–593
20. Cantor C. R., and Schimmell P. R. (1980) *Biophysical Chemistry,* pp. 849–866, W. H. Freeman and Co., San Francisco
21. Myers, J. K., Pace, C. N., and Scholtz, J. M. (1995) *Protein Sci.* **4,** 2138–2148
22. Kuwajima, K (1989) *Proteins* **6,** 87–103
23. Ptitsyn O. B., Pain, R. H., Semisotnov, G. V., Zerovnik, E., and Razgulyaev O. I. (1990), *FEBS Lett.* **262,** 20–24
24. Silva, J. L., Foguel, D., and Royer, C. A. (2001) *Trends Biochem. Sci.* **26,** 612–618
25. Royer, C. A. (2002) *Biochim. Biophys Acta* **1595,** 201–209
26. Pryse, K. M., Bruckman, T. G., Maxfield, B. W., and Elson, E. L. (1992) *Biochemistry* **31,** 5127–5136
27. Kobashigawa, Y., Sakurai, M., and Nitta, K. (1999) *Protein Sci.* **8,** 2765–2772
28. Vidugiris, G. J. A., and Royer, C. A. (1998) *Biophys. J.* **75,** 463–470
29. Inoue, K., Yamada, H., Akasaka, K., Herrmann, C., Kremer, W., Maurer, T., Doker, R., and Kalbitzer, H. R. (2000) *Nat. Struct. Biol.* **7,** 547–550
30. Frye, K. J., and Royer, C. A. (1998) *Protein Sci.* **7,** 2217–2222
31. Rashin, A. A., Iofin, M., and Honig, B. (1986) *Biochemistry* **25,** 3619–3625
32. Williams, M. A., Goodfellow, J. M., and Thornton, J. M. (1994) *Protein Sci.* **3,** 1224–1235
33. Hubbard, J. S., Gross, K. H., and Argos, P. (1994) *Protein Eng.* **7,** 613–626
34. Srinivasulu, S., and Appu Rao, A. G. (1996) *Biochim. Biophys. Acta* **1294,** 115–120
35. Malvezzi-Campeggi, F., Rosato, N., Finazzi-Agrò, A., and Maccarrone, M. (2001) *Biochem. Biophys. Res. Commun.* **289,** 1295–1300
36. Ford-Hutchinson, A. W., Gresser, M., and Young, R. N. (1994) *Annu. Rev. Biochem.* **63,** 383–417
37. Finazzi Agrò, A., Avigliano, L., Egmond, M. R., Veldink, G. A., and Vliegenthart, F. G. (1975) *FEBS Lett.* **52,** 73–76
38. Klein, B. P., Cohen, B. S., Grossman, S., King, D., Malovany, H., and Pinsky, A. (1985) *Phytochemistry*, **24,** 1903–1906

39. Boyington, J. C., Gaffney, B. J., and Amzel, L. M. (1993) *Science* **260,** 1482–1486
40. Sudharshan, E., Srinivasulu, S., and Appu Rao, A. G. (2000) *Biochim. Biophys. Acta* **1480,** 13–22
41. Millar, D. P. (1996) *Curr. Opin. Struct. Biol.* **6,** 637–642
42. Wasylewski, Z., Koloczek, H., Wasniowska, A., and Slizowska, K. (1992) *Eur. J. Biochem.* **206,** 235–242
43. Mei, G., Pugliese, L., Rosato, N., Toma, L., Bolognesi, M., and Finazzi-Agrò, A. (1994) *J. Mol. Biol.* **242,** 559–565
44. Di Venere, A., Mei, G., Gilardi, G., Rosato, N., De Matteis, F., McKay, R., Gratton, E., and Finazzi-Agrò, A. (1998) *Eur. J. Biochem.* **257,** 337–343
45. Brand, L., and Gohlke, J. R. (1972) *Annu. Rev. Biochem.* **41,** 843–868
46. Arighi, C. N., Rossi, J. P., and Delfino, J. M. (1998) *Biochemistry,* **37,** 16802–16814
47. Jenkins, A. E., Hockenberry, J. A., Nguyen, T., and Bernlohr, D. A. (2002) *Biochemistry,* **41,** 2022–2027
48. Sudharshan, E., and Appu Rao, A. G. (1997) *FEBS Lett.* **406,** 184–188
49. Ramachandran, S., Carroll, R. T., Dunham, W. R., and Funk, M. O. (1992) *Biochemistry* **31,** 7700–7706
50. Gillmor S. A., Villasenor, A., Fletterick, R., Sigal, E., and Browner, M. F. (1997) *Nat. Struct. Biol.* **12,** 1003–1009
51. Hemak, J., Gale, D., and Brock, T. G. (2002) *J. Mol. Model.* **8,** 102–112
52. Maccarrone, M., Taccone-Gallucci, M., Meloni, C., Cococcetta, N., Manca di Villahermosa, S., Casciani, U., and Finazzi-Agrò, A. (1999) *J. Am. Soc. Nephrol.* **10,** 1991–1996
53. Maccarrone, M., Van Zadelhoff, G., Veldink, G. A., Vliegenthart, J. F. G., and Finazzi-Agrò, A. (2000) *Eur. J. Biochem.* **267,** 5078–5084
54. Carlile, A. J., Bindschedler, L. V., Bailey, A. M., Bowyer, P., Clarkson, J. M., and Cooper, R. M. (2000) *Mol. Plant Microbe Interact.* **13,** 538–550
55. Rusterucci, C., Montillet, J. L., Agnel, J. P., Battesti, C., Alonso, B., Knoll, A., Bessoule, J. J., Etienne, P., Suty, L., Blein, J. P., and Triantaphylides, C. (1999) *J. Biol. Chem.* **274,** 36446–36455